

Project Mountain Valley Sunshine—Progress in Science and Technology

NORIIHIKO FUKUTA

Department of Meteorology, University of Utah, Salt Lake City, Utah

(Manuscript received 18 October 1994, in final form 16 January 1996)

ABSTRACT

In order to improve the cloud seeding reaction, the basic processes in cloud microphysics and dynamics were critically examined. The disadvantage of the large temperature dependence in heterogeneous ice nucleation, as well as the advantage of there being almost no temperature dependence of strong coolants in homogeneous ice nucleation, was pointed out. A new horizontal seeding method using liquid carbon dioxide has been devised to maximize the effects of seeding, and simple devices for airborne and ground mobile applications were developed and tested in supercooled fogs and low-lying stratus clouds. Seeding tests revealed the development of vertical motions of the seeded plume and associated wind, the effective mixing of the plume with the surrounding supercooled fog and cloud volume, the resultant development of large crystals and their fall, the enlargement of the initial opening, the associated snowfall and its effects on traffic, and the accompanying optical effects. The developed ground mobile fog seeding method was found to be practical. A fundamental feedback reaction of the seeded plume at or near the overlying stabilization zone, which we call FILAS (falling-growth induced lateral air spreading), has been identified as an effective mechanism to cause precipitation in a large fog and cloud volume. Cellular motions and accompanying pseudoadiabatic lapse rates were confirmed in the fog and cloud.

1. Introduction

Mountain valleys at midlatitudes, those in the western United States in particular, frequently develop supercooled fogs in winter (Hill 1988), which substantially reduce the amount of sunshine reaching the ground and cause various problems. Considering the essential requirements for achieving the maximum seeding effects—that is, sufficient number of ice particles near 0°C, the condition and the time duration of ice crystal growth sustained by a slowly rising but rapidly diffusing ice crystal plume laid by a horizontally moving ice crystal source—a bare bones project of seeding liquid carbon dioxide (LC) in supercooled fog, dubbed Mountain Valley Sunshine (MVS), was designed and started in the mid-1980s with the hope that significant supercooled fog clearing and greatly enhanced sunshine at the ground would not only lead to beneficial results but would also clarify fundamental seeding processes as well as the fog structure and properties. The project is an elaboration of Project Sunshine suggested earlier by Schaefer (1975), with an emphasis on detection and delineation of new seeding reaction, postponing detailed studies such as those of Meyer et al. (1986) until the future. The remarkable seeding effects observed during the early airborne tests have

already been reported (Fukuta 1989). Since then, for practical reasons, the project has developed a ground mobile seeding capability using LC. The new seeding method resulted in an even larger scale, easily recognizable, and highly reproducible physical effect and also elucidated MVS fog characteristics and seeding reactions, including recognition of a fundamental and self-enhancing mechanism of the seeding effect. In this paper, we shall report the scientific and technological progress made by the project.

2. Properties of supercooled fogs in mountain valleys

In preparation for the seeding tests, properties of the supercooled fogs in the Salt Lake (SL) Valley were carefully examined. Figure 1 shows the profiles of the air temperature and the dewpoint depression ΔT_d on a fog day (26 December 1985) and a no-fog day (7 January 1986) measured at the SL airport (1.29 km MSL). On the fog day, the air remains near $\Delta T_d = 0^\circ\text{C}$ up to about 500 m, the fog top. The temperature lapse rate is very close to pseudoadiabatic, suggesting that a warmed parcel can rise to the fog top where it will stop due to the layer of strong temperature inversion above. In the layer, $\Delta T_d \approx 0$ tells of the existence of saturated water vapor and/or fog throughout the day. The temperature of the fog layer is below 0°C and the fog is supercooled. The temperature excursion between 0500 and 1700 MST is less than 2°C and is observed in the entire layer. This suggests the effect of sunshine re-

Corresponding author address: Dr. Norihiro Fukuta, Department of Meteorology, University of Utah, 819 Wm. C. Browning Building, Salt Lake City, UT 84112.

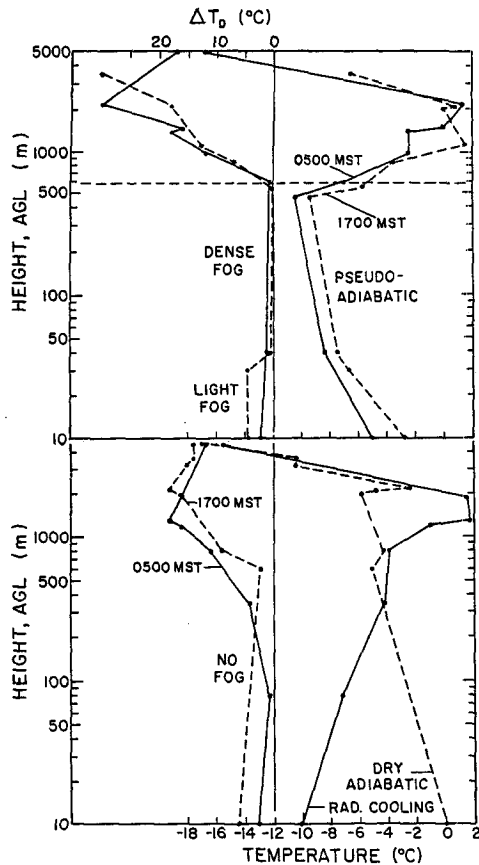


FIG. 1. Temperature and dewpoint depression ΔT_d profiles on a fog day (26 December 1985, top) and a no-fog day (7 January 1986, bottom) at the Salt Lake airport. The fog top is at around 500 m AGL, and the mountain tops are at about 2 km AGL.

flection at the fog top. On a typical foggy day, at ground level it is dark and chilly. On the other hand, on the no-fog day, ΔT_d moves away from 0° and the temperature near the ground at 0500 MST becomes substantially lower due to radiative cooling both in the valley and on the slopes of the mountains. The latter causes downslope transport of cold air. This profile changes into a dry-adiabatic lapse rate by 1700 MST, an indication of dry air convection caused by heating due to the sunshine. The daytime temperature increases above the values on a foggy day, but at night the temperature becomes slightly lower than that on the foggy day. Fog begins to develop as high pressure dominates the region, and its depth increases as this condition continues.

Figure 2 shows the wind profile at the SL airport on both foggy and dry days. The profile is basically the same regardless of fog formation, with the speed less than 2 m s^{-1} . However, the directions are opposing between the layer above the mountain range (approximately 2 km AGL) and that near the ground, the former normally being northwesterly. This variation of the

wind direction, or a gentle rotation with the axis in the horizontal direction, is apparently caused by friction between the prevailing wind above the mountain range and the cooler valley air.

The winter fogs in the mountain valleys induce various problems and hazards, which are summarized in Fig. 3. Besides the obvious visibility problems at airports and on highways, the low temperature in the fog leads to increases in home heating fuel consumption, accompanying air pollution generation, and health hazards.

3. Design of seeding processes

Careful evaluation of basic processes involved in seeding, as well as their effective application, is crucial for obtaining desirable effects. This was the motivation for the present seeding project.

a. Microphysical and dynamical considerations

1) CHOICE OF ICE NUCLEANT

Ice nucleation is the first reaction that takes place during the seeding. There are basically two main mech-

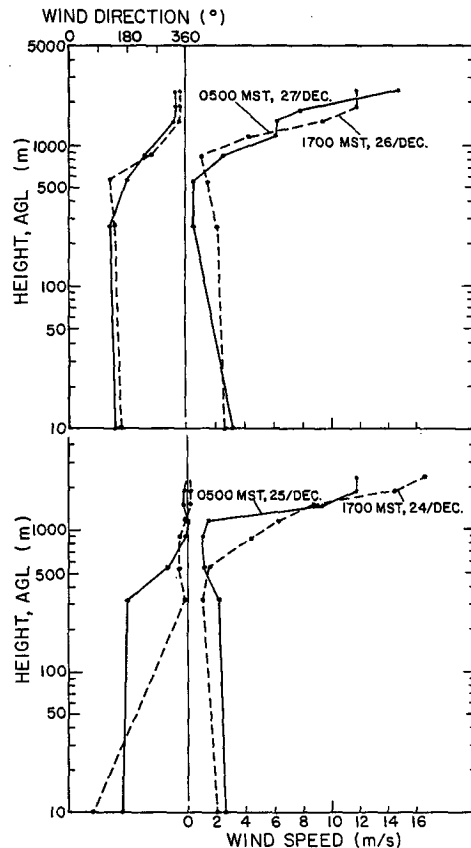


FIG. 2. Wind profiles on fog days (26–27 December 1985, top) and no-fog days (25–26 December 1985, bottom) in Salt Lake Valley.

FOG AND THE PROBLEMS

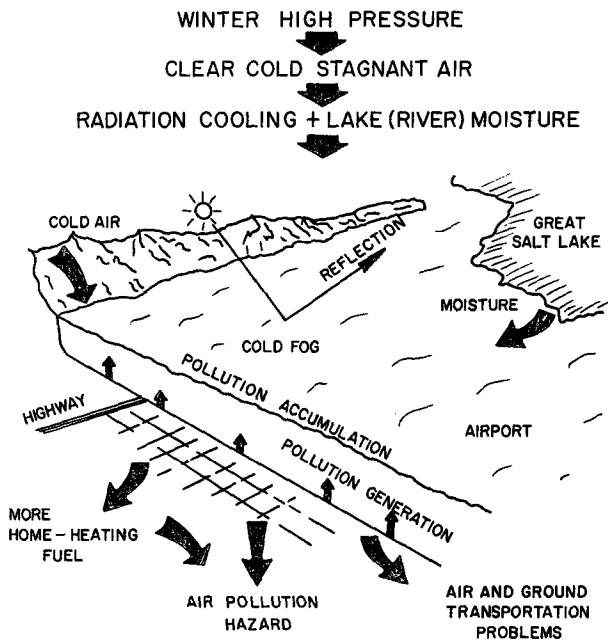


Fig. 3. Fog and the associated problems in the Salt Lake Valley.

anisms of ice nucleation—the homogeneous and the heterogeneous. The former generates ice crystals by strong cooling (typically provided by dry ice), and the latter by lowering the energy barrier of new phase formation using ice forming nuclei such as silver iodide (AgI). Apart from details of heterogeneous ice nucleation mechanisms, they show a large difference in the number of ice particles nucleated for a given mass of compound at temperatures below but approaching 0°C, the former far greater than the latter. The second notable feature is that the number of ice crystals generated by the coolant is nearly independent of the temperature. Figure 4 shows a comparison between the number of ice crystal generations per gram of dry ice and the number for AgI on the basis of equal total mass output; for AgI, this is the total mass of the 2% solution. The number of ice crystal generations per gram of LC is basically the same as that of dry ice and is probably close to the maximum the homogeneous mechanism can achieve (Fukuta 1988). The surface temperature of dry ice drops to -100°C when pellets are falling (Fukuta et al. 1971; Fukuta 1987), and that of sprayed LC drops to -90°C (Fukuta 1965).

2) ICE CRYSTAL GROWTH PARAMETERS

Ice crystals generated by the seeding grow if they are placed among supercooled droplets and/or supersaturated air. The mass of ice crystals growing within a cloud of supercooled droplets is shown in Fig. 5. The

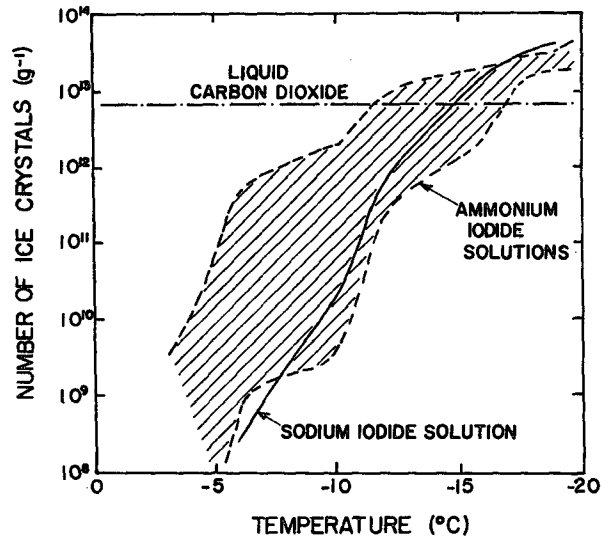


Fig. 4. Comparison of activity spectra between dry ice (Fukuta et al. 1971, with correction) and the smoke of silver iodide airborne generators (Garvey 1975). The latter is based on the weight of the 2% solution used. The activity of liquid carbon dioxide is basically the same as that of dry ice.

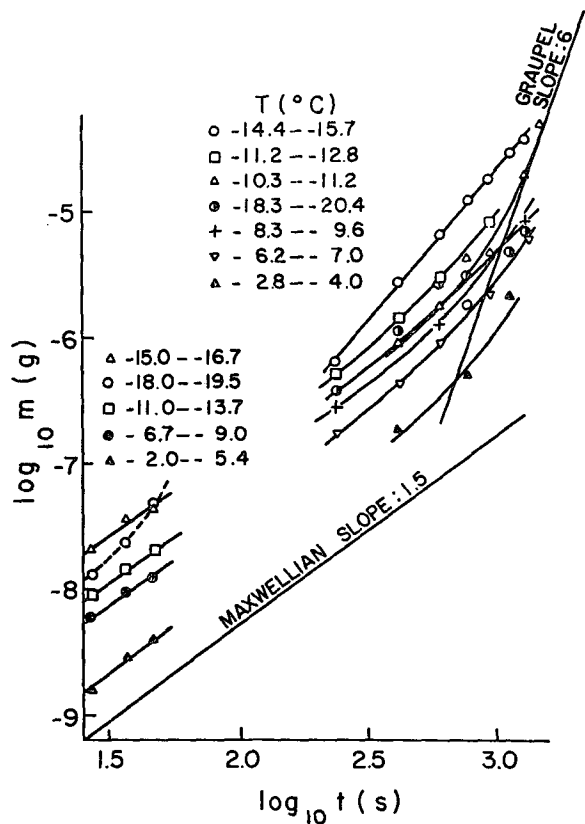


Fig. 5. Ice crystal mass m plotted as a function of growth time t at different temperature T (Fukuta et al. 1984).

mass of the crystals grown by the vapor diffusion mechanism varies less than approximately one order of magnitude in the temperature range from -2° to -20°C within the time period of less than, say, 10^3 s. If the crystals grow, they develop fall velocity and fall. The fall distance of ice crystals growing among the supercooled droplets is given in Fig. 6. In about 30 min, ice crystals grown at temperatures around -10°C fall about 750 m, while those growing at other temperatures approximately fall about 350–450 m, except near 0°C . In addition, during the growth, ice crystals generate the heat of phase change that contributes to the buoyancy of the plume. This heat is close to the latent heat of fusion, but as the process approaches its end due to the exhaustion of supercooled droplets, a further adjustment becomes necessary to reach a thermodynamic equilibrium by changing the condition of vapor phase, and the extent varies depending on the liquid water content (Fukuta 1973). This heating is the origin of the added buoyancy in the ice crystal plume. The buoyancy has the remarkable feature that, unlike a hot plume, which loses its buoyancy as it diffuses and cools down, the temperature of the ice crystal plume always stays higher than that of the surrounding supercooled droplets, and therefore, the buoyancy is sustained at the same level as long as it remains glaciated. The warmed condition stays in the parcel even when the ice crystals are all precipitated out. This buoyancy leads to an enhanced ice crystal plume spreading, as we shall discuss in the next section. The plume of ice nuclei before activation does not show this effect, and the turbulent diffusion is no more than that of the ordinary smoke.

Thus, although ice crystal growth factors mentioned above are applicable only to isolated ice crystals in the supercooled environment and behaviors of ice crystals in the seeded plume are somewhat different, the growth factors for a given period of time within the temperature range of seeding, including the mass, fall velocity, and heat generation, vary roughly within one order of magnitude, whereas the ice nucleation factor—that is, the active number of ice nucleants per unit mass of material—varies drastically depending on the temperature in the case of heterogeneous ice nucleants but not for the homogeneous ice nucleants. The nearly constant number of ice crystal generation by LC, regardless of the fog or cloud temperature as long as it is below 0°C , gives distinct advantages over heterogeneous nuclei in the design of seeding procedures. Specifically, there is no need for seeding rate adjustment with temperature and faster turbulent diffusion of the plume.

3) MICROPHYSICS—PLUME DIFFUSION INTERACTION

In regard to ice crystal growth, the dynamic condition of the ice crystal plume is important. The growth behaviors mentioned above are based on crystals that are surrounded by a sufficient number of supercooled droplets and are, therefore, the fastest. To grow ice

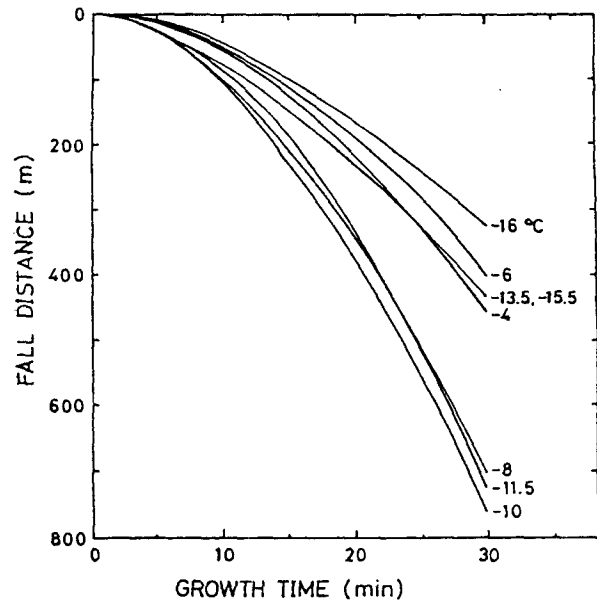


FIG. 6. Variation of fall distance with time at various temperatures (Takahashi and Fukuta 1988).

crystals efficiently in the seeded plume, at least the following two conditions must be satisfied simultaneously: first, *ice crystal plume diffusion into or mixing with a large volume of supercooled cloud or fog*, and second, *a sufficient duration of the time*. The heterogeneous ice nucleant plume simply diffuses under the influence of an existing eddy field before ice nucleation. On the other hand, the ice crystal plume generated by homogeneous ice nucleants or coolants tends to spread more due to the addition of its own upward motion in the existing eddy field of the cloud with the buoyancy caused by the heat of phase change. While the buoyancy of a given cloudy air parcel is determined by the thermodynamic as well as the microphysical conditions (Fukuta 1973), the actual force that acts to the parcel depends on its orientation critically affecting the mode of spreading. The orientation of the buoyant parcel further influences the time duration for its ascent and the dynamic stabilization at the end of the process. A vertically generated ice crystal plume (e.g., by dropping a dry-ice pellet) tends to cause an organized rapid upward motion of the plume (Kraus and Squires 1947) due to vertical integration of the buoyant force. Commonly in these cases, the time for the plume diffusion and ice crystal growth is too short. Due to the small size of ice crystals produced in this way, they are often called gushing “smoke” by commercial seeders for airport fog clearing. This overseeding effect has also been confirmed by the observation of dry-ice-seeded ice crystals moving horizontally. Furthermore, such an ice crystal plume stabilizes when it reaches the bottom of the temperature inversion or the end of its upward motion, and due to the lack of turbulent mixing and the

small ice crystal size, a further interaction with the supercooled cloud or fog parcel below is severely restricted. In this regard, a horizontally laid ice crystal plume avoids the vertical force integration and rises relatively slowly, yet it creates a motion like the cumulus cell and provides sufficient time for the turbulent mixing and entrainment with surrounding supercooled cloud or fog. This also satisfies the requirement of time for ice crystal growth and the condition that ice crystals be mixed with supercooled droplets. Toward the end of the plume rise, ice crystals become large enough to fall and enter into the fresh low-lying supercooled cloud or fog volume for continuing growth. Considering these physical properties of LC and other practical ones such as its low price (about half that of dry ice), nontoxicity, safety to the environment (Cooper and Jolly 1970; Klein 1978), nonflammability, lack of asphyxiating fumes in the cockpit unlike dry ice, convenience of long-term storage, continuous and accurate discharging as a liquid with a vapor pressure (52 atm at 15°C), and high ice nucleation efficiency, LC was chosen for horizontal penetration seeding at an altitude slightly higher than the 0°C isotherm for the airborne seeding and along the ground with a car-based device.

4) SEEDING RATE

The seeding rate of LC was roughly determined by the following two methods. In 20 min, ice crystals under isolated growth will fall a distance $\Delta z = 200\text{--}400$ m (cf. Fig. 6) and the mass $m_c = 10^{-5}$ g (cf. Fig. 5). Assuming the liquid water content $W_L = 1$ g m⁻³ and number of ice crystal generations by LC $n = 10^{13}$ g⁻¹, the mass of LC necessary to treat V m³ of the cloud or fog volume

$$m_{CO_2} = \frac{W_L V}{n m_c} \tag{1}$$

For $V = 1$ km³, the LC mass required $m_{CO_2} \approx 10$ g.

The second method is based on the volume of ice crystal plume expected to diffuse in 20 min along the length u of 1-s flight. Assuming the fall distance in the period to be Δz , the horizontal width of the plume spread perpendicular to the direction of seeding as Δy , the amount of LC to be discharged in the same period of time is given by

$$P = \frac{u \Delta z \Delta y W_L}{n m_c} \tag{2}$$

For $u \approx 100$ m s⁻¹, $\Delta z \approx 300$ m, $\Delta y = 2000$ m, and $P = 0.6$ g s⁻¹. This corresponds to a 10 g mile⁻¹ (6 g km⁻¹) seeding rate. Considering one order of magnitude uncertainty in some values used in the above estimation, the actual seeding rate was taken to be about 25 times larger, or 250 g mile⁻¹ (155 g km⁻¹), and occasionally to be another factor of 2 larger. These seeding rates are considerably smaller than the conven-

tional seeding rate of dry ice. The 250 g mile⁻¹ seeding rate corresponds to 15 g s⁻¹ LC discharging with the aircraft speed at 200 kt (370 km h⁻¹) and corresponds to 2 g s⁻¹ for a car speed of 30 mile h⁻¹ (50 km h⁻¹). The rate applies regardless of the temperature due to the constancy of factors involving LC ice nucleation behavior and ice crystal growth.

5) VISIBILITY

The effect of seeding on fog visibility and, therefore, on the sunshine transmission is twofold: 1) change from many small fog droplets to few large crystals and 2) the ice crystal fallout.

When the ice crystals grow by evaporating fog droplets, the process proceeds under approximate conservation of the mass of the condensed phases—that is, water and ice. The meteorological visual range V_m (or sunlight penetration) is inversely proportional to the product between the number concentration n and the cross-sectional area of spherical particles of radius r (Johnson 1963):

$$V_m \propto \frac{1}{nr^2} \tag{3}$$

From the mass conservation, assuming the density remains roughly the same,

$$n \propto \frac{1}{r^3} \tag{4}$$

Then,

$$V_m \propto \frac{1}{nr^2} \propto r \propto \left(\frac{1}{n}\right)^{1/3} \tag{5}$$

The fall velocity w of the ice crystals in question obeys the so-called Stokes law under the condition of seeding, or

$$w \propto r^2 \propto \frac{1}{n^{2/3}} \tag{6}$$

From these two relationships, it becomes immediately clear that formation of larger crystals is advantageous for an increase in visibility.

b. Seeding devices

1) AIRBORNE SEEDING

An LC cylinder rack mountable on a seeding aircraft was developed (see Fig. 7). The design has been approved by the Federal Aviation Administration. The LC cylinder, made of aluminum, has a 50-lb (23 kg) LC capacity and weighs 23 kg when dry. The cylinder rack weighs 36 kg and the base 14 kg. Three hollow cone spray nozzles, designed for agricultural use, with 5, 8, and 12 g s⁻¹ discharging rates were mounted un-

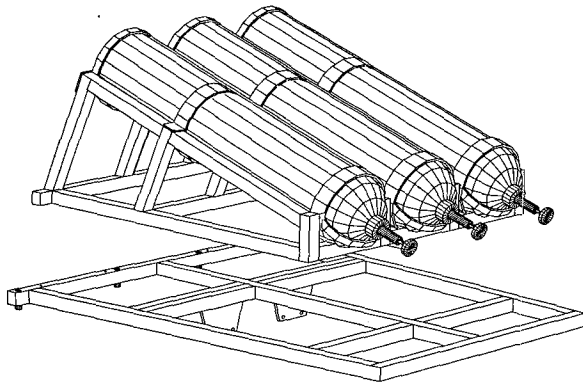


FIG. 7. Liquid carbon dioxide tank rack system developed for airborne use. It is made of 1.5-in. (3.8 cm) square aluminum tubing, the rack is 114 cm (along the cylinder length) \times 96.5 cm, and the height to the top of cylinder is 60 cm. The base outer dimensions are 141 cm \times 117 cm.

der the aircraft body and used in combination with LC spraying into the backward direction of the flight.

2) GROUND SEEDING

Two systems were developed for ground seeding. Stationary LC discharging devices with timers were made with the cooperation of the Utah Department of Transportation. Use revealed a serious difficulty in targeting the seeding effect with varying wind directions, and the cost of the facility did not meet the economic requirement. Consequently, this system has been abandoned. The second system is based on a simple LC spraying device mountable on a car (see Fig. 8). It consists of LC cylinders (aluminum) and a spray nozzle system mounted on either a ski rack or a luggage rack. The cylinder holds 50 lb (23 kg) of LC and is placed in the rack with the valve side on the lower end. A copper pipe of 0.25-in. (6.35 mm) o.d. was used to lead the LC to the nozzle, whose diameter is 0.25 mm for a 2 g s^{-1} output of LC. The height of the nozzle is adjusted within the legal limit of the maximum vehicle height (14 ft or 4.3 m). A later version uses a foldable nozzle support on a sedan with 20-lb (9.1 kg) capacity LC cylinders in a smaller rack. This system provides excellent preparedness for seeding. This design is convenient for parking the car in a garage and for nozzle service, which is needed occasionally. The seeding car is also equipped with a digital monitoring thermometer using a cabled probe and a citizens band radio for communication.

c. Seeding method

Prior to the seeding, the subfreezing temperature of the fog requires confirmation. The seeding effect appears normally within 15 min of the time of seeding but takes a progressively longer time as the temperature

approaches 0°C due to slower ice crystal growth (Takahashi and Fukuta 1988; Takahashi et al. 1991).

1) AIRBORNE SEEDING

Prior to the actual penetration seeding in fog, a leg of the same length was flown at the fog top and in the same direction planned for the seeding runs. Then after returning to the starting position, penetration seeding was carried out at varying depths in the same direction for the same period of time, normally 2 min. Seeding direction was north-south most of the time to make the detection of seeded crystal plumes easy in the morning sun. Sites along the side of Stansbury Island or Antelope Island, both oriented approximately in a north-south direction, were often used with the islands as the landmark. Considering the danger from various protrusions from the ground, sites within the city were avoided and tests were done over the Great Salt Lake, but only after it was confirmed that the fog bottom was sufficiently above the lake surface prior to the test.

The qualitative physical effects to be detected within the seeded area are optical effects (a part of a sun pillar), increased clarity or visibility, and the increasing size of the hole as a function of time. The width of the hole was measured by flying the aircraft above it and documenting the traverse time and the air speed.

2) GROUND SEEDING

Mobile seeding was carried out either by seeding on a upwind road with a time distance of about 20 min from the target area or by seeding around the target by selecting a time distance so that a portion of the seeded and widened plume reached the target even under the

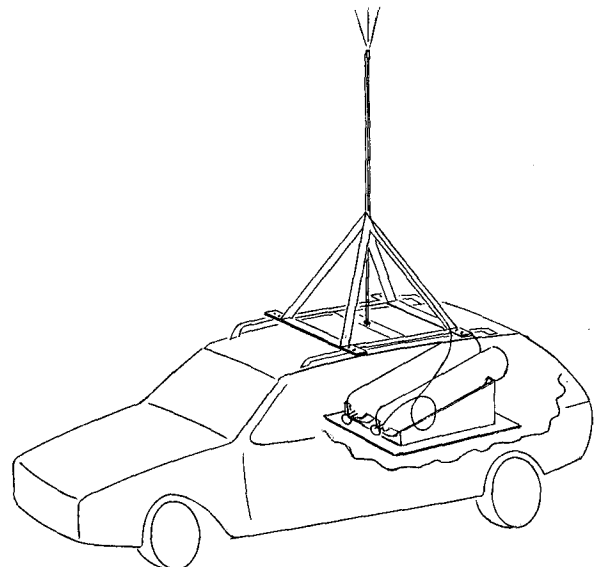


FIG. 8. A simple LC spraying device mountable on a car.

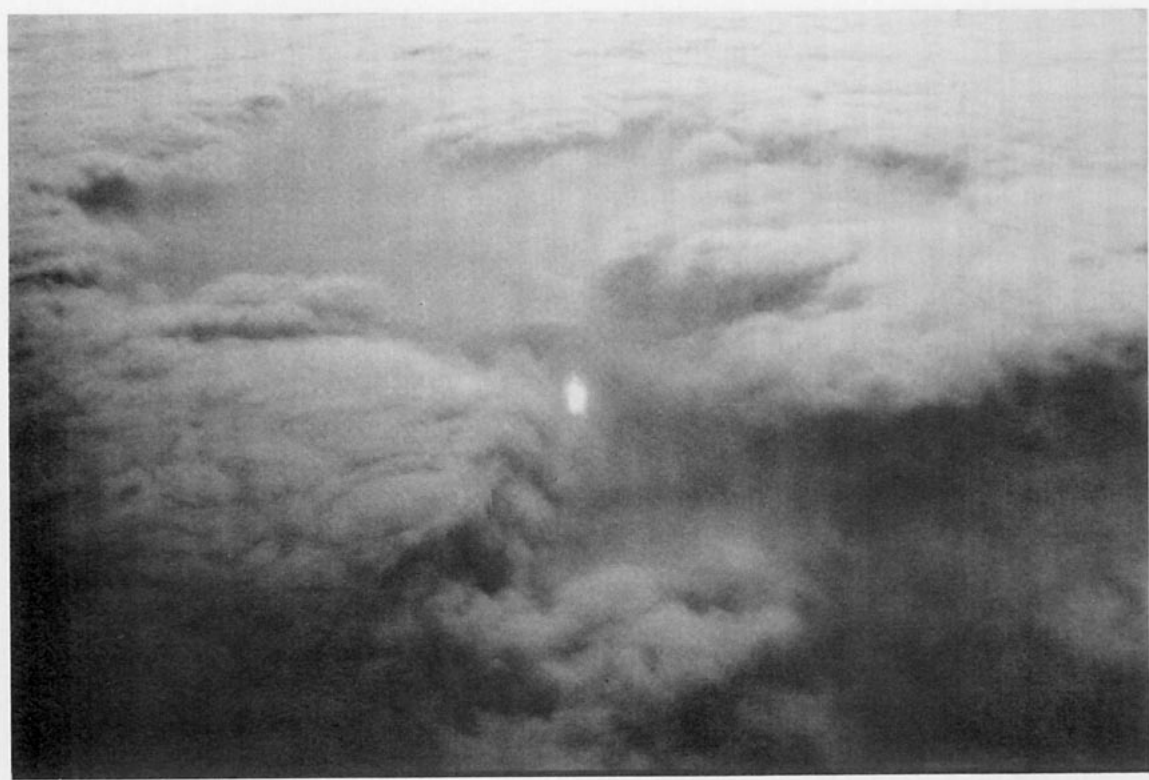


FIG. 9. Bright spot—that is, a part of sun pillar, and the hole developed after an airborne penetration seeding (0948–1020 MST) where $T = -7^{\circ}\text{C}$ east of Stansbury Island on 28 January 1988. The maximum width of the hole is about 4 km, and the cellular motion of the fog is recognizable.

varying wind. This is particularly effective for seeding an airport or a dangerous section of highway. When the bottom of the fog does not reach the ground, a mountainside road in the fog, if available, can be seeded, as shown later.

4. Results and discussion

a. Airborne seeding

In the winter of 1987/88 over the southern part of the Great Salt Lake, three penetration seeding tests were carried out using a simple LC discharging device under cooperation with industrial partners, Intermountain Air College and Sorex. In all cases, the fog was approximately 300 m thick and the LC discharging rate was about 10 g s^{-1} .

The first seeding test was performed on 29 December 1987 at a site immediately east of Stansbury Island. During the first period of seeding, from 1051 to 1056 MST, the fog temperature was -6°C , and during the second period, from 1120 to 1124 MST, -4°C . The second test was on the morning of 28 January 1988 from 0930 to 1200 MST in four tracks at sites between Stansbury Island and Antelope Island with the fog-top temperature at -7°C . The seeding effect was clearly

identified based on a distinct optical effect (a portion of a sun pillar) from the artificial ice crystals and the visual sinkhole (see Fig. 9). The optical effect was not as complete as that reported by Hobbs and Radke (1975), the latter being seeded very heavily with dry ice resulting in smaller ice crystals. The width of the opening reached 2 km in about 30 min, and the lake surface became visible. From the pattern of the seeded hole and appearance of the fog top, it became clear that the fog consists of convective cells in which the seeding effect took place. This is different from the static structure of fog considered in Dennis (1980) but is in good agreement with the pseudoadiabatic lapse rate determined by the sounding (see Fig. 1). The visibility achieved in this test seeding was far better than that in the dry-ice seeding that was being carried out at the Salt Lake International Airport where our seeding aircraft took off. The seeding rate was 300 g LC km^{-1} .

b. Ground seeding

Stationary automated ground seeding was carried out in the winter of 1989/90 at three locations in Salt Lake City. The seeding effect was examined by driving a car on roads surrounding the seeding generator at a distance of about 1 km in the early morning. Seeded ice



FIG. 10. Symmetric parhelia from seeded ice crystals where $T = -9^{\circ}\text{C}$, an Orem, Utah, on the morning of 19 January 1992.

crystals were easily recognizable with associated good visibility in the fog under the car headlights, but targeting the seeding effect onto the intended area caused serious problems. For this reason, the mobile mode of seeding evolved.

The mobile ground seeding method was tested in Vernal, Utah, fog on the morning of 23 February 1990. The seeding was done on a highway U.S. 40 location, which showed a sharp turn, and an opening in the shape of the turn with a portion of undersun was recognized from the airborne observations. The fog temperature was -8°C at the beginning of seeding.

Applying the mobile seeding devices shown in Fig. 8, supercooled fogs in Salt Lake City and the vicinity were seeded extensively during the winter of 1991/1992 at airports, freeways, cities, and other foggy places, with 29 cases in all during early morning and evening hours. Fog temperatures were mostly warmer than -10°C , with a few occasions as low as -13°C . A slowly developing seeding effect was observed in a fog with temperatures as high as -1°C . Fog depth was normally less than 100 m with variable visibility. The area cleared using one or two cars was often several tens of square kilometers. For targeting the seeding effect onto the dangerous section of highway under the varying wind, seeding around it a couple of times at about a distance of a few kilometers normally cleared the

whole area covering several tens of square kilometers. Once the entire Salt Lake Valley area covering 10^3 km^2 was cleared by four cars seeding in the morning hours. Currently this seeding method is in practice at the Salt Lake International Airport and Boise (Idaho) airport.

Seeding effects were always easily confirmed visually. The timing of ice crystal appearance, the direction, fresh snowfall, and drastic visibility improvement, accompanied by falling ice crystals, in addition to beautiful optical effects such as parhelia (see Fig. 10), sun (light) pillar or undersun, were used to judge the effect. Recent snowfall from the seeding was obvious due to the presence of very few tire marks and was normally a few millimeters deep. It did not make the road slick and tended to be blown away by the wakes of cars. Nighttime seeding is particularly revealing. Car headlights clearly illuminate the falling ice crystals with accompanying optical effects, often light pillars. During nighttime seeding without the help of solar radiation, the opening appeared to enlarge for a while, even after ice crystals had entirely fallen out and stars become visible. Wind frequently develops sometime after the start of seeding. The tendency for the hole created in the fog to close was not strong even during nighttime seeding. This was presumably because the temperature lowering had mostly occurred by the time seeding ended and the fog formation process weakened. In the daytime seeding,

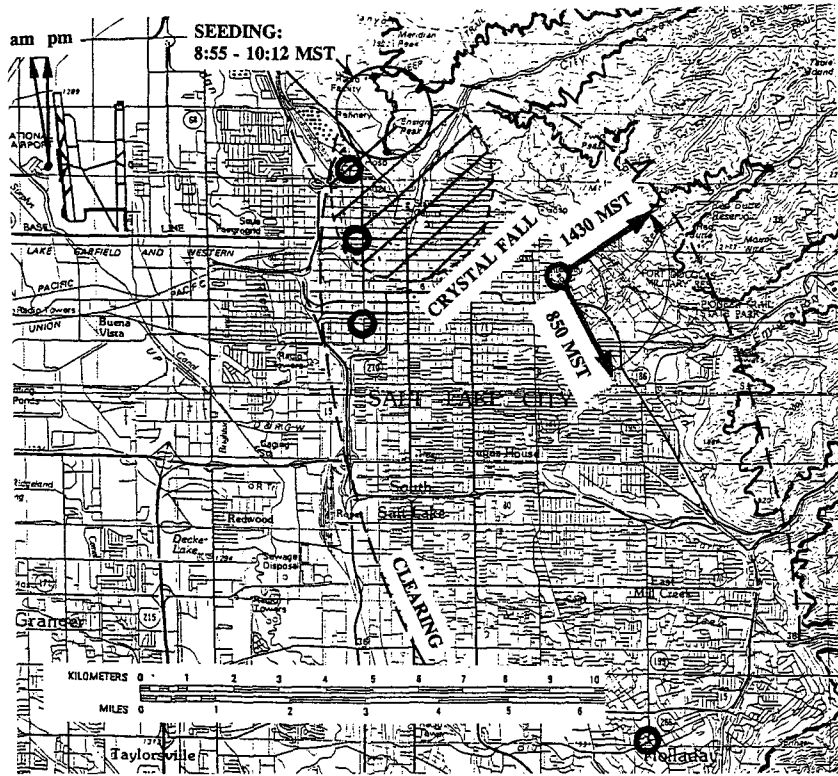


FIG. 11. Seeding of a bottom-lifted fog on Ensign Peak Road on 27 December 1991. Here, $T = -4.3^{\circ}$ to -2.9°C , there are four seeding cycles, and the total LC consumption is 20 lb (9.1 kg). Circles show the locations where clearing was observed.

which normally starts in the morning, the hole not only never closed but also continued to enlarge due to the heating effect of the sunshine introduced. Closing, however, did happen sometimes after the sun set.

When the fog temperature was below 0°C , the seeded ice crystal plume always rose, indicating the dominating effect of phase change heat generation, and went out of sight. It took normally between 10 and 15 min before ice crystals falling back to the ground were detected.

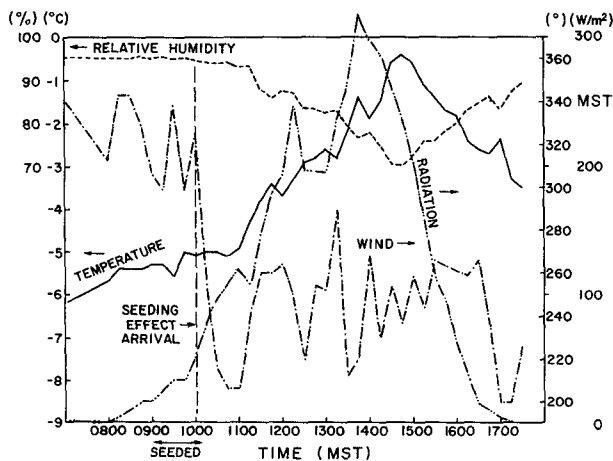


FIG. 12. Meteorological data measured at the University of Utah upon arrival of seeded opening on 27 December 1991.

On occasion, a fog developed with the bottom lifted from the valley floor, making the normal ground mobile seeding impossible. Such a fog or low-lying stratus can be seeded from a road high on a mountain slope. Figure 11 shows such an example of seeding bottom-lifted supercooled fog on 27 December 1991. At the time of seeding, the wind was clearly northwesterly, and repeated seeding was done from 0855 to 1012 MST with 9 kg of LC on a 2-km stretch of mountain road. Fresh snow cover was observed on the downwind road southeast of the seeding location shortly after the end of seeding. At the foothill site of the University of Utah, 5 km downwind of the seeding location at about 1000 MST, the estimated time of arrival of the seeding effect, the wind direction, the solar radiation, the temperature, and the relative humidity all started changing (see Fig. 12). Particularly remarkable was the change of wind from a direction parallel to the Wasatch Mountain Range to one perpendicular to it, as seen in Figs. 11

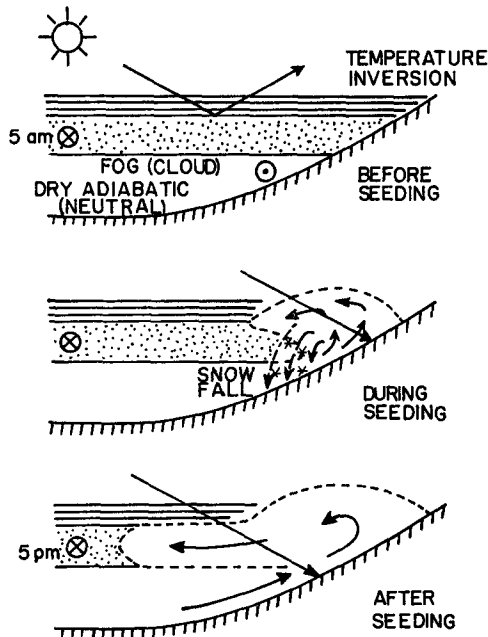


FIG. 13. Estimated effects of seeding and additional sunshine on the bottom-lifted fog on 27 December 1991.

and 12. This change may be compared to the steady wind throughout the day at the Salt Lake International Airport adjacent to the southeast corner of the Great Salt Lake. The seeding reaction estimated to have occurred is shown in Fig. 13. The solar radiation introduced by the seeding apparently caused a major up-draft, which kept pushing the fog layer away from the mountain range and maintained the insolation until sunset.

c. Fog characteristics revealed

As has been anticipated from the sounding data, cellular patterns observed from aircraft, and the rapid rise

of seeding plume, there exist cellular structures of convective motion in the fog, and when the seeded cell has been destroyed, adjacent cells become clearly visible.

d. Falling-growth induced lateral air spreading (FILAS)

The seeding study revealed an effective supercooled cloud and fog modification mechanism. Glaciation of supercooled clouds and fogs causes additional buoyancy, as discussed above. In order to achieve high quality fog clearing, the ice crystals must fall out after growth, and for the growth, mixing or entrainment of the supercooled fog into the ice crystal plume is needed. Such a process takes time, and a slow rise of the plume is required. The rise of the plume is driven by the buoyancy force, and the force can integrate vertically. This is to say that in order to create a slow-rising plume with sustained shear for effective turbulent diffusion and mixing, the plume should be laid horizontally to avoid the vertical integration of the buoyant force or rapid plume rise.

The top of a fog or a cloud often rests at a stable boundary like the bottom of a temperature inversion. It was discovered that if such a supercooled fog or cloud is seeded by the method described above, the buoyant ice crystal plume rises and spreads horizontally after reaching the boundary. However, the ice crystals thus grown possess sufficient size to fall into the underlying supercooled fog or cloud, and additional buoyant air created below rises, which causes further lateral spreading of the plume. This falling-growth induced lateral air spreading (FILAS, see Fig. 14), a feedback mechanism, provides an effective way to spread the falling ice crystals rapidly at the top of supercooled fog or cloud over a wide area and allows them to convert the supercooled water into falling ice crystals by a diffusional growth mechanism, enabling them to modify a large fog or cloud volume. The horizontal seeding of a homogeneous ice nucleant like LC at the bottom of such a layer makes the mechanism most effective, and

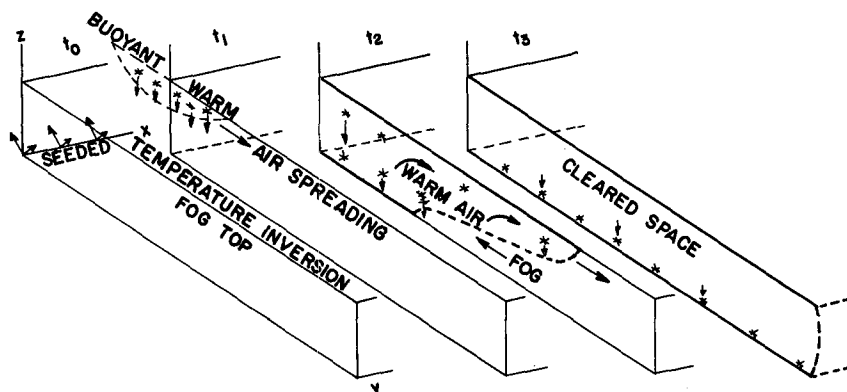


FIG. 14. Illustration of the falling-growth induced lateral air spreading (FILAS) mechanism.

this seeding method should also be applicable to other modes of ice phase weather modification.

5. Conclusions and summary

Project MVS has so far clarified the following.

By examining characteristics of ice nucleants and ice crystal growth parameters, it has been shown that the strong temperature dependence of the active number per unit mass of heterogeneous ice nucleants presents a serious disadvantage in designing the basic processes of cloud seeding. In this regard, the nearly temperature-independent number of homogeneous ice nucleants or coolants gives a distinct advantage.

By analyzing the interaction between ice crystal plume generated by a homogeneous ice nucleant and the surrounding supercooled fog or cloud volume, the horizontal orientation of the plume is shown to better satisfy the ice crystal growth condition—that is, a sufficiently long period of time under the condition constantly mixed with supercooled fog or cloud volume.

Considering the practical and technical requirements of seeding, LC was chosen, and airborne as well as ground mobile devices were developed and tested, with the results exceeding initial expectations.

The results of seeding tests in supercooled fog and low stratus clouds include growth and fallout of ice crystals, better visibility and a much larger cleared area than achieved by conventional airborne dry ice seeding, and the associated dynamic effects, including wind development and optical effects. In fog seeding, snowfall did not lead to slick road conditions, and the wide area cleared permitted introduction of sunshine to the ground, which evaporated any snowfall during the daytime. No closing of the opening was observed before sunset. Clearing of an area as wide as several tens of square kilometers was achieved in a few hours by one car with temperatures below about -3°C . Fog clearing was recorded at fog temperatures as warm as -1°C , although much more slowly.

Under the varying wind, a method of directing the seeding effect in the fog over the target area has been developed—that is, mobile ground seeding around the target area.

The effect of sunshine introduced to the ground by seeding was definite. On the slope of a mountain, a 90° wind direction change from parallel to the mountain range to perpendicular was observed with an increase in insolation and temperature and a decrease in relative humidity. Updraft induced by introduced sunshine pushes the fog away at the bottom of the temperature inversion and maintains the opening.

A new fundamental seeding reaction, which we call FILAS, has been identified in which the fall of large ice crystals out of the seeded plume when reached at the bottom of a stable layer causes continuing growth-

induced heating in the fog below and subsequent rise of the air. This rising air effectively spreads the plume horizontally over a wide area of supercooled fog or clouds and helps the remaining ice crystals to fall, grow, and treat a large volume in a feedback manner.

The project revealed the existence of convective cells in the fog and low-lying stratus cloud and their pseudoadiabatic temperature profile, which permits the seeded plume to rise and reach the top.

Acknowledgments. This work was supported by the Division of Atmospheric Sciences, National Science Foundation, under Grants ATM 8616568 and 9112888; Geneva Steel Company; Utah Energy Office; and Morris Air.

REFERENCES

- Cooper, C. F., and W. C. Jolly, 1970: Ecological effects of silver iodide and other weather modification agents. A review. *Water Resour. Res.*, **6**, 88–89.
- Dennis, A. S., 1980: *Weather Modification by Cloud Seeding*. Academic Press, 267 pp.
- Fukuta, N., 1965: Production of ice crystals in air by a pressure-pack method. *J. Appl. Meteor.*, **4**, 454–456.
- , 1973: Thermodynamics of cloud glaciation. *J. Atmos. Sci.*, **30**, 1645–1649.
- , 1987: The surface temperature of dry ice, solid CO_2 . *J. Wea. Mod.*, **19**, 99–101.
- , 1988: The maximum rate of homogeneous ice nucleation in air by cooling. *Proc. 12th Int. Conf. on Nucleation and Atmospheric Aerosols*, Vienna, Austria, 504–507.
- , 1989: Project Mountain Valley Sunshine. *Fifth WMO Scientific Conf. on Weather Modification and Applied Cloud Physics*, Beijing, China, World Meteorological Organization, 505–508.
- , W. A. Schmeling, and L. F. Evans, 1971: Experimental determination of the ice nucleation by falling dry ice pellets. *J. Appl. Meteor.*, **10**, 1174–1179.
- , N.-H. Gong, and A.-S. Wang, 1984: A microphysical origin of graupel and hail. *Proc. Ninth Int. Cloud Physics Conf.*, Tallinn, U.S.S.R., 257–260.
- Garvey, D. M., 1975: Testing of cloud seeding materials at the Cloud Simulation and Aerosol Laboratory, 1971–1973. *J. Appl. Meteor.*, **14**, 883–890.
- Hill, G. E., 1988: Fog effect of the Great Salt Lake. *J. Appl. Meteor.*, **27**, 778–783.
- Hobbs, P. V., and L. F. Radke, 1975: The nature of winter clouds and precipitation in the Cascade Mountains and their modification by artificial seeding. Part II: Techniques for the physical evaluation of seeding. *J. Appl. Meteor.*, **14**, 805–818.
- Johnson, J. C., 1963: *Physical Meteorology*. MIT Press, 393 pp.
- Klein, D. A., 1978: *The Environmental Impacts of Artificial Ice Nucleating Agents*. Dowden, Hutchinson and Rose, 257 pp.
- Kraus, E. B., and P. Squires, 1947: Experiments on the stimulation of clouds to produce rain. *Nature*, **159**, 489–491.
- Meyer, M. B., G. G. Lala, and J. E. Juisto, 1986: FOG-82: A cooperative field study of radiation fog. *Bull. Amer. Meteor. Soc.*, **67**, 825–832.
- Schaefer, V. J., 1975: Project Sunshine. *J. Wea. Mod.*, **7**, 1–3.
- Takahashi, T., and N. Fukuta, 1988: Supercooled cloud tunnel studies on the growth of snow crystals between -4 and -20°C . *J. Meteor. Soc. Japan*, **66**, 841–855.
- , T. Endoh, G. Wakahama, and N. Fukuta, 1991: Vapor diffusional growth of free-falling snow crystals between -3 and -23°C . *J. Meteor. Soc. Japan*, **69**, 15–30.